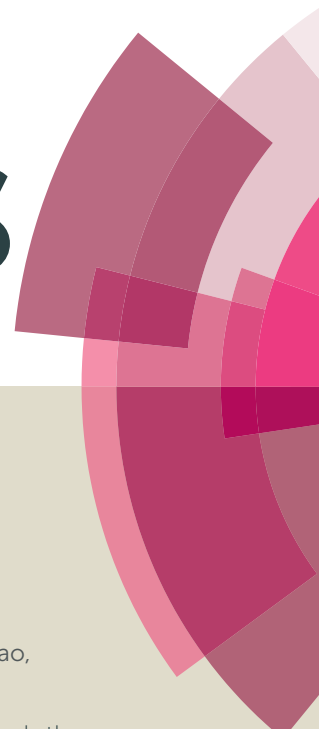


RSC Advances



This article can be cited before page numbers have been issued, to do this please use: B. Zhang, T. Zhao, J. Zhou, Q. Qiu, Y. Dai, M. Pan, W. Huang and H. Qian, *RSC Adv.*, 2016, DOI: 10.1039/C6RA02405J.



This is an *Accepted Manuscript*, which has been through the Royal Society of Chemistry peer review process and has been accepted for publication.

Accepted Manuscripts are published online shortly after acceptance, before technical editing, formatting and proof reading. Using this free service, authors can make their results available to the community, in citable form, before we publish the edited article. This *Accepted Manuscript* will be replaced by the edited, formatted and paginated article as soon as this is available.

You can find more information about *Accepted Manuscripts* in the [Information for Authors](#).

Please note that technical editing may introduce minor changes to the text and/or graphics, which may alter content. The journal's standard [Terms & Conditions](#) and the [Ethical guidelines](#) still apply. In no event shall the Royal Society of Chemistry be held responsible for any errors or omissions in this *Accepted Manuscript* or any consequences arising from the use of any information it contains.

**Design, synthesis and biological evaluation of novel triazole-core reversal agents
against P- glycoprotein-mediated multidrug resistance**

Bo Zhang ^a, Tianxiao Zhao ^a, Jie Zhou ^a, Qianqian Qiu ^a, Yuxuan Dai ^a, Miaobo Pan ^a,
Wenlong Huang ^{a, b, *} and Hai Qian ^{a, b, *}

Abstract

We designed and synthesized a novel series of P-glycoprotein (P-gp)-mediated multidrug resistance (MDR) inhibitors bearing a triazolphenethyl-tetrahydroisoquinoline scaffold through click chemistry. Then those synthesized compounds were tested on doxorubicin-resistant erythroleukemia K562/A02 cells in a series of experiments. The result is that most of the synthesized compounds exhibits more active MDR reversal activity than verapamil (VRP). However, among them, compound **11** exhibits less cytotoxicity (IC_{50} s > 100 μ M), but more potency than the known P-gp inhibitor WK-X-34 and VRP on increasing anticancer drug accumulation in K562/A02 cells. Moreover, this compound can not only persist longer chemo-sensitizing effect (>24h) than VRP (<6h) with reversibility, but also significantly reverse MDR in a dose-dependent manner. Therefore, considering the low intrinsic cytotoxicity but strong reversal activity in vitro, compound **11** may be a promising lead with a potent and safe resistance modulator in combinational cancer chemotherapy.

1 Introduction

Tumor chemotherapy is a most important tool in the treatment of metastatic cancer. However, drug resistance is regarded as the major barrier to successful chemotherapy in cancer patients, a phenomenon known as multidrug resistance (MDR) ^[1, 2]. The resistance to therapy is caused by the over-expression of membrane-associated transport proteins named ATP-binding cassette (ABC) transporters including P-glycoprotein (P-gp/ABCB1), breast cancer resistance protein (BCRP/ABCG2), and multidrug resistance protein 1 (MRP/ABCC1), which has been recognized as resulting in the increased efflux of chemotherapeutic drugs from cancer cells ^[3, 4]. Among them, P-glycoprotein (P-gp) plays the most critical role in MDR ^[5], which is a 170-kDa plasma membrane protein encoded by the MDR1 gene ^[6]. To overcome MDR, using specific inhibitors to direct inhibition of P-gp should be regarded as a suitable and attractive approach ^[7].

During the past three decades, in order to reverse the MDR in cancer cells, three generations of P-gp inhibitors have been developed such as Verapamil ^[8], VX-710 ^[9], Zosuquidar (LY335979 ^[10] and Tariquidar (XR9576) ^[11] (**Fig. 1**). However, because of many factors, none of the P-gp inhibitors has been approved for clinical application, such as unsatisfactory toxicity, low selectivity, poor potency or adverse pharmacokinetic interaction with anticancer drugs ^[12, 13], which also lead to that, up to now, no P-gp inhibitor has been approved by regulatory agencies ^[14]. Therefore, the discovery of safe and effective P-gp inhibitors still remains to be a huge challenge in this field.

For designing novel P-gp inhibitors with high activity and low toxicity, we selected the tetrahydroisoquinolinethylphenylamine-based P-gp inhibitor WK-X-34 as a lead compound, which was designed and synthesized by researchers from the University of Bonn through CADD (Computer-Aided Drug Design) and methodical combinatorial chemistry. WK-X-34 is one of the third-generation of P-gp inhibitors, which not only exhibits little competitive effect against combination therapy drugs, but also shows relative high cytotoxicity ($IC_{50} < 10 \mu\text{M}$)^[15]. Therefore, through click chemistry method, amide group is replaced by 1, 2, 3-triazole ring, which is a hydrophobic aromatic group, and can associate with biological targets through hydrogen bonding (**Fig. 2**)^[6, 17]. Click chemistry, which commonly employs the 1, 3-dipolar cycloaddition combined with the synthetic design of triazoles and tetrazoles, has been widely applied in drug discovery^[18]. On the basis of principles above, we designed and synthesized a series of P-gp-mediated MDR reversal agents. Herein, we report the biological activity of newly synthesized P-gp-mediated MDR reversal agent.

2 Chemistry

Compounds **1-12** were prepared starting from 2-nitrophenol and 3, 4-dimethoxyphenethylamine, and the synthetic routes of target compounds were outlined in **Scheme 1**. Firstly, 2-nitrophenol and 3-bromo-1-propyne were refluxed in the mixture of acetone and potassium carbonate for 4h affording compound **a**. Secondly, compound **a** reacted with ammonium chloride in the presence of iron

powder in 80% ethanol affording compound **b**, which then reacted with freshly formed aromatic acyl chloride and triethylamine in dry dichloromethane to give compounds **c1-c12**. Compounds **d** and **e** were synthesized according to literature procedures with minor modification ^[16]. Subsequently, compounds **e** reacted with sodium azide affording compound **f**. Last, compound **f** reacted with diverse alkyne **c1-c12** through click chemistry to provide compounds **1-12**. The structures of target compounds obtained were listed in **Table 1**.

3 Results and discussion

3.1 Cytotoxicity of the target compounds

To identify ideal P-gp inhibitors reversing MDR at non-toxic concentrations, MTT (3-(4, 5-dimethylthiazolyl-2)-2, 5-diphenyltetrazolium bromide) assay was adopted to evaluate the intrinsic cytotoxicity of the target compounds against the human erythroleukemia K562 cells and the adriamycin (ADM)-resistant K562/A02 cells, which shows MDR due to P-gp overexpression (induced by ADM) and has been proved as useful in the quantification and characterization of MDR reversal by modulators of the MDR phenotype ^[19, 20]. We chose verapamil (VRP) as the positive control, which is a well-known classical P-gp inhibitor. As shown in **Table 1**, the majority of the target compounds displays low intrinsic cytotoxicity since their IC₅₀ values are at a high micromolar level. As expected, K562/A02 cells are significantly resistant to ADM: K562/A02 (IC₅₀ for ADM of 71.04 ± 3.2 μM) displaying about 151.9-fold higher than K562 cells (IC₅₀ of 0.47 ± 0.03 μM). In contrast, compound **5**

and **7** is found to exhibit high toxicity ($IC_{50} < 25 \mu\text{M}$) in both cell lines, VRP has weak cytotoxic effect toward K562 and K562/A02 cells with IC_{50} values 41.6 and 37.2 μM and WK-X-34 displaying a high level of toxicity toward K562 cells (IC_{50} of $6.9 \pm 1.9 \mu\text{M}$) but a weak toxicity toward K562/A02 cells (IC_{50} of $33.7 \pm 2.7 \mu\text{M}$). Based on the IC_{50} s, most of target compounds possess low cytotoxicity in tested cell lines and are suitable candidates for the development of P-gp inhibitors.

3.2 Effects of the target compounds on reversing ADM resistance in K562/A02 cells

Based on the preliminary experiment, most of target compounds possess low cytotoxicity in tested cell lines. The reversal effects of target compounds on the MDR phenotype have been examined in K562/A02 cells at 0.5 μM -concentrations by MTT assay. As the results summarized in **Table 2**, anticancer drug ADM alone displays little inhibitory effect on the survival of K562/A02 cells (IC_{50} of $71.04 \pm 3.2 \mu\text{M}$). However, the reversal fold (RF) data indicates that all target compounds and VRP increase the inhibitory effect of different doses. It reveals that all of the target compounds possess MDR reversal activity. Moreover, most of the target compounds exhibits more active MDR reversal activity than the classical P-gp inhibitor VRP, when co-administered with ADM at the same condition. Notably, compound **11** shows the strongest reversal activity among the synthesized compounds (IC_{50} of $1.76 \pm 0.3 \mu\text{M}$).

3.3 Chemo-sensitizing effect of target compounds

Based on the results of preliminary experiments, we selected the most potent

compound **11** for further study. To further investigate the reversal potency and dose–response effects, the cytotoxicity of ADM against K562/A02 cells (P-gp-overexpression) was evaluated in the presence of the compound **11** at various concentrations (0.10 μM , 0.25 μM , 0.50 μM , 1.00 μM , 2.50 μM , 5.00 μM , 10.00 μM , 20.00 μM) by MTT assay ^[21]. As the results summarized in **Table 3**, compound **11** showed apparent dose dependent activity and still exhibited potent MDR reversal activity (RF = 4.6) when the concentration decreased to 1.00 μM . Additionally, the EC₅₀ value of compound **11** was 488.5 ± 71.2 nM (**Fig. 3**), which was analyzed by GraphPad Prism 5.0 software from the dose–response curves. Those results indicated that compound **11** significant potentiated the cytotoxicity of ADM in K562/A02 cells in a dose-dependent manner.

3.4 Duration of MDR reversal effect of compound 11 toward ADM in K562/A02 cells

It is known that an ideal P-gp inhibitor should possess a relatively long duration of action with reversibility for safe and effective therapy of P-gp-mediated MDR cancers ^[22]. Therefore, we used VRP and WK-X-34 as positive controls to evaluate the duration of MDR reversal effect of compound **11**. The experiment was executed as previous report with minor modification ^[21]. K562/A02 cells were incubated with 5 μM of compound **11**, VRP and WK-X-34 for 24h, and then we washed compounds with PBS (phosphate buffered saline). At different time points (0, 6, 12 or 24h), after removing the compounds, we added ADM in various concentrations to the culture, and incubated for additional 48 h. The results, examined by MTT assay, were shown

in **Table 4**: after pre-incubation with VRP, WK-X-34 and compound **11**, the IC_{50} s of ADM towards K562/A02 cells were 19.32 μ M, 2.32 μ M, 2.11 μ M respectively (no wash group). The MDR-reversing effect of VRP (RF = 1.6) waned immediately after its removal from the medium and totally disappeared after 6h. In contrast, compound **11** and WK-X-34 showed a very strong reversal activity even after removed from the medium for 24h, and the IC_{50} s of ADM were 32.41 μ M (RF = 2.5) and 12.91 μ M (RF = 6.2), respectively. Moreover, compound **11** displayed potent chemo-sensitizing effect and persisted for longer time compared with the positive control VRP. The data also indicated that the MDR reversal effect of compound **11** towards K562/A02 cells was reversible.

3.5 Accumulation of ADM

Furthermore, in order to investigate the compound **11** can reverse P-gp-mediated drug efflux, we selected ADM as a fluorescent probe, which was a fluorescent substrate of P-gp and could be used to monitor drug accumulation in cells ^[23], and measured the fluorescence intensity of ADM through spectrofluorometry according to the previous report with minor modification. As shown in **Fig. 4**, the P-gp inhibitor VRP and WK-X-34 were selected as positive controls. The ADM-sensitive K562 cells retained most of the fluorescence ADM, while the P-gp-overexpressing K562/A02 cells showed comparatively low intracellular level of ADM. The fluorescence intensity of ADM in K562/A02 cells, treated with compound **11**, VRP or WK-X-34, was obviously increased in a dose-dependent

manner. In comparison, Compound **11** showed a higher level of ADM accumulation than VRP at the same dose, and has similar reversal activity compared with WK-X-34. The results indicated that compound **11** exhibited similar potency with WK-X-34 at different concentrations and more potent than VRP in inhibiting the ADM transport activity of P-gp.

3.6 Inhibitory effect of compound **11** on P-gp efflux function

In order to further validate our assumption, we selected rhodamine-123 (Rh123) as another fluorescent probe, which was a well-known fluorescent substrate of P-gp and could be used to investigate whether compound **11** could reverse P-gp-mediated drug efflux by targeting P-gp. It is known that P-gp transporter can rapidly reduce Rh123 in the intracellular accumulation through an increase of Rh123 efflux from cells, which overexpresses on the adriamycin-selected K562/A02 cells. The level of Rh123 was measured by monitoring its fluorescence intensity through flow cytometry assay according to the method described in literatures with minor modification ^[24, 25]. As shown in **Fig. 5**, the P-gp inhibitor VRP and WK-X-34 were selected as positive controls. The adriamycin-sensitive K562 cells retained most of the fluorescence Rh123, while the P-gp-overexpressing K562/A02 cells showed comparatively low intracellular level of Rh123. In comparison, treated with compound **11**, VRP or WK-X-34, the fluorescence intensity of Rh123 in K562/A02 cells was obviously increased in a dose-dependent manner. Particularly, compound **11** showed a higher level of Rh123 accumulation than VRP at the same dose, and had

similar reversal activity compared with WK-X-34. The results indicated that compound **11** was targeting p-gp and could effectively block the drug efflux.

4 Conclusions and Future Directions

In summary, we selected WK-X-34 as a lead compound, and twelve compounds were newly designed and synthesized based on the click chemistry. All synthesized compounds were evaluated in vitro for MDR chemo-sensitizing effects by using the classical P-gp inhibitor VRP as a positive control. Most of target compounds possessed low cytotoxicity and exhibited more active MDR reversal activity than VRP, especially for Compound **11**, which showed the strongest reversal activity and could effectively prevent the ADM efflux function of P-gp and increased the accumulation of ADM in K562/A02 cells. Therefore, compound **11** could be served as a promising candidate to develop P-gp-mediated MDR reversal modulator in cancer chemotherapy and further intensive investigations are still in progress.

5 Experimental section

5.1 General chemistry

All reagents and solvents were reagent grade and were used without further purification unless otherwise stated. Column chromatography was carried out on silica gel or alumina (200 – 300 mesh). Melting points were measured using a Mel-TEMP II melting point apparatus, which was uncorrected. All of the target compounds were analyzed by ^1H NMR, ^{13}C NMR (Bruker ACF-300Q, 300 MHz), MS

(1100 LC/MSD spectrometer; Hewlett–Packard) and IR (Nicolet Impact 410); Thin-layer chromatography (TLC) was performed on GF/UV 254 plates and the chromatograms were visualized under UV light at 254 and 365 nm. Compounds **d** and **e** were prepared as previously described ^[16]. The starting compound 2-nitrophenol was commercially available.

5.2 Synthesis of 1-Nitro-2-(prop-2-yn-1-yloxy) benzene (**a**)

The mixture of 2-nitrophenol (11.2 g, 80 mmol), 3-bromoprop-1-yne (9.52 g, 80 mmol), and potassium carbonate (22.1 g, 160 mmol) in acetone (120 mL) was heated to reflux for 3 h. The reaction mixture was cooled to 0 °C followed by filtration and concentration to afford 12.6 g compound **a**. Yield: 89.1%. Yellow powder, m.p.: 66–68 °C.

5.3 Synthesis of 2-(Prop-2-yn-1-yloxy) aniline (**b**)

The mixture of **a** (12.4 g, 70 mmol), ammonium chloride (18.7 g, 350 mmol) and iron powder (11.7 g, 210 mmol) in 80% ethanol (150 mL) was heated to reflux for 3.5 h. After cooling to room temperature, the mixture was adjusted with sodium carbonate to PH = 7–8, filtered with Celite, and concentrated under vacuum to afford a brown residue. Dichloromethane (50 mL) was added into the residue and the resulted solution was washed by saturated aqueous Na₂CO₃ (30 mL) and brine (30 mL) in sequence. The organic layer was dried by anhydrous Na₂SO₄. The solvent was evaporated to afford 8.40 g compound **b** as brown oil. Yield: 81.7%.

5.4 General procedure for the preparation of **c1–c12**

Synthesis of **c3**, **c6**, **c8**: to the solution of compound **b** (0.74g, 5 mmol) and triethylamine (0.84g, 6 mmol) in dichloromethane (20 mL), heterocyclic aromatic acyl chloride (5 mmol) in dichloromethane (15 mL) was added at 0 °C, and then, the mixture was stirred at room temperature for 24 h. The reaction solution was washed by 3% hydrochloric acid (2 × 20 mL), saturated aqueous Na₂CO₃ (20 mL), and brine (20 mL) in sequence. The organic layer was dried by anhydrous Na₂SO₄. The solvent was evaporated to afford the desired product **c3**, **c6** and **c8**. Synthesis of other compounds: to the solution of compound **b** (0.74g, 5 mmol) and heterocyclic aromatic formic acid (5 mmol) in dichloromethane (20 mL), EDC·HCl (1.44 g, 7.5 mmol) in dichloromethane (15 mL) was added, and then, the mixture was stirred at room temperature for 24 h. The reaction solution was washed by 3% hydrochloric acid (2 × 20 mL), saturated aqueous Na₂CO₃ (20 mL), and brine (20 mL) in sequence. The organic layer was dried by anhydrous Na₂SO₄. Then, filtered and evaporated to afford the desired product compound **c1–c12**. Yield: 45.7%–86.3%

5.5 Synthesis of 2-(4-Azidophenethyl)-6,7-dimethoxy-1,2,3,4-tetrahydroisoquinoline (**f**)

Compound **e** (1.9 g, 6.1 mmol) was dissolved in 50% acetic acid (30 mL). To this solution, sodium nitrite (0.6 g, 8.5 mmol) was slowly added at -5 to 0 °C within 30 min. The solution was vigorously stirred at 0–5 °C for 50 min. Sodium azide (0.6 g, 9.2

mmol) was batch added into the reaction mixture at 0–5 °C. The resulting solution was stirred at 0–5 °C for 1 h followed by diluting with ice water (200 mL) and extracting with EtOAc (3 × 100 mL). The combined organic layer was washed with water (2 × 60 mL), saturated aqueous NaHCO₃ (2 × 60 mL) and brine (2 × 50 mL), dried over anhydrous Na₂SO₄, filtered and concentrated to afford 1.2 g pink solid. Yield 58.2%. m.p.: 68–70 °C

5.6 General procedure for the preparation of compounds 1–12

To the solution of **c1–c12** (1 mmol) and **f** (1 mmol) in 75% methanol (40 mL), ascorbate sodium (30 mg) and CuSO₄ (10 mg) were added, respectively. The reaction solution was stirred at room temperature for 24–48 h. After filtration, the solvent was evaporated and the crude product was purified by silica gel column chromatography using a mixture of ethylacetate/ Methanol (15:1, v/v) as eluent to give the desire product with high purity. The purity of each tested compounds (>95%) was determined on a Waters UPLC/MS instrument using a Waters C18 column (1.7 μm 2.1× 50 mm, with a flow rate of 0.2 mL/min and detection at 254 nm) employing a 10–90% acetonitrile/water/0.1% formic acid gradient.

5.6.1

N-(2-((1-(4-(2-(6,7-dimethoxy-3,4-dihydroisoquinolin-2(1H)-yl)ethyl)phenyl)-1H-1,2,3-triazol-4-yl)methoxy)phenyl)picolinamide (1)

Yield 62.3%; white powder; mp: 164–165 °C. ¹H NMR (300 MHz, DMSO-*d*₆) δ:

10.52 (s, 1H, CONH), 8.94 (s, 1H, NCH=C), 8.58 (d, $J = 3.2$ Hz, 1H, ArH), 8.45 (d, $J = 7.5$ Hz, 1H, ArH), 8.17 (d, $J = 7.4$ Hz, 1H, ArH), 8.03-8.11 (m, 1H, ArH), 7.78 (d, $J = 7.8$ Hz, 2H, ArH), 7.63 (d, $J = 5.1$ Hz, 1H, ArH), 7.49 (d, $J = 7.7$ Hz, 2H, ArH), 7.39 (d, $J = 7.8$ Hz, 1H, ArH), 7.15-7.05 (m, 2H, ArH), 6.64 (d, $J = 7.5$ Hz, 2H, ArH), 5.45 (s, 2H, OCH₂), 3.70 (s, 6H, 2 × OCH₃), 3.32 (s, 2H, ArCH₂N), 2.90-2.71 (m, 8H, 4 × CH₂); ¹³C NMR (75 MHz, DMSO-*d*₆) δ: 152.7, 151.3, 148.2, 147.6, 146.7, 144.4, 139.4, 137.5, 134.8, 134.8, 134.0, 128.2, 127.7, 127.7, 126.8, 126.7, 126.5, 124.2, 122.1, 121.2, 120.3, 119.1, 112.8, 111.4, 108.0, 72.3, 59.7, 58.0, 56.3, 56.1, 33.4, 27.3; ESI-MS *m/z*: 590.7 [M+H]⁺; IR (KBr, cm⁻¹) ν: 3321.63, 1682.10, 1253.90 (-CONH-), 2926.25, 1227.37 (-OCH₃), 1601.04, 1533.16, 1519.15, 1454.96, 759.28, 689.13.

5.6.2

N-(2-((1-(4-(2-(6,7-dimethoxy-3,4-dihydroisoquinolin-2(1H)-yl)ethyl)phenyl)-1H-1,2,3-triazol-4-yl)methoxy)phenyl)isonicotinamide (2)

Yield 72.9%; white powder; mp: 112-114 °C; ¹H NMR (300 MHz, DMSO-*d*₆) δ: 9.84 (s, 1H, CONH), 8.82 (s, 2H, ArH), 7.86 (s, 2H, ArH, NCH=C), 7.73 (d, $J = 8.2$ Hz, 4H, ArH), 7.48 (d, $J = 8.3$ Hz, 2H, ArH), 7.38 (d, $J = 8.1$ Hz, 1H, ArH), 7.25 (t, $J = 7.1$ Hz, 1H, ArH), 7.04 (d, $J = 7.5$ Hz, 1H, ArH), 6.64 (d, $J = 8.0$ Hz, 2H, ArH), 5.34 (s, 2H, OCH₂), 3.70 (s, 6H, 2 × OCH₃), 3.55 (s, 2H, ArCH₂N), 2.93-2.70 (m, 8H, 4 × CH₂); ¹³C NMR (75 MHz, DMSO-*d*₆) δ: 164.7, 152.7, 149.7, 148.2, 146.7, 144.4, 140.8, 139.4, 134.8, 134.8, 134.0, 128.2, 127.7, 127.7, 126.8, 126.5, 124.2, 121.7, 121.7, 121.2, 120.3,

119.1, 112.8, 111.4, 108.3, 72.3, 59.7, 58.0, 56.3, 56.1, 56.1, 33.4, 27.3; ESI-MS m/z : 591.4 $[M+H]^+$; IR (KBr, cm^{-1}) ν : 3410.09, 1666.55, 1257.70 (-CONH-), 2938.05, 1226.55 (-OCH₃), 1599.35, 1540.60, 1519.05, 1452.51, 1129.59, 750.87.

5.6.3

N-(2-((1-(4-(2-(6,7-dimethoxy-3,4-dihydroisoquinolin-2(1H)-yl)ethyl)phenyl)-1H-1,2,3-triazol-4-yl)methoxy)phenyl)furan-2-carboxamide (3)

Yield 56.1%; brown powder; mp: 136-138 °C; ¹H NMR (300 MHz, DMSO-*d*₆) δ : 9.16 (s, 1H, CONH), 8.90 (s, 1H, NCH=C), 7.97 (d, J = 7.9 Hz, 1H, ArH), 7.88 (s, 1H, ArH), 7.82 (d, J = 8.2 Hz, 2H, ArH), 7.52 (d, J = 8.3 Hz, 2H, ArH), 7.36 (d, J = 8.1 Hz, 1H, ArH), 7.29 (d, J = 3.3 Hz, 1H, ArH), 7.17 (t, J = 6.7 Hz, 1H, ArH), 7.01 (t, J = 7.7 Hz, 1H, ArH), 6.74 (s, 1H, ArH), 6.70-6.68 (m, 2H, ArH), 5.39 (s, 2H, OCH₂), 3.98 (s, 2H, ArCH₂N), 3.72 (s, 6H, 2 × OCH₃), 3.33-2.73 (m, 8H, 4 × CH₂); ¹³C NMR (75 MHz, DMSO-*d*₆) δ : 162.7, 152.7, 148.2, 148.2, 146.7, 144.4, 143.8, 139.4, 134.8, 134.8, 134.0, 128.2, 127.7, 127.7, 126.8, 126.5, 124.2, 121.2, 120.3, 119.1, 115.3, 112.8, 111.7, 111.4, 108.3, 72.3, 59.7, 58.0, 56.3, 56.1, 56.1, 33.4, 27.3. ESI-MS m/z : 580.9 $[M+H]^+$; IR (KBr, cm^{-1}) ν : 3404.13, 1655.59, 1254.53 (-CONH-), 2932.15, 1227.88 (-OCH₃), 1583.32, 1538.77, 1518.35, 1452.78, 1130.76, 755.12.

5.6.4

N-(2-((1-(4-(2-(6,7-dimethoxy-3,4-dihydroisoquinolin-2(1H)-yl)ethyl)phenyl)-1H-1,2,3-triazol-4-yl)methoxy)phenyl)furan-3-carboxamide (4)

Yield 59.0%; brown powder; mp: 143-145 °C; ^1H NMR (300 MHz, $\text{DMSO-}d_6$) δ : 9.22 (s, 1H, CONH), 8.83 (s, 1H, NCH=C), 8.38 (s, 1H, ArH), 7.78-7.72 (m, 4H, ArH), 7.49 (d, $J = 8.4$ Hz, 2H, ArH), 7.35 (d, $J = 8.0$ Hz, 1H, ArH), 7.19 (t, $J = 7.2$ Hz, 1H, ArH), 7.03-6.95 (m, 2H, ArH), 6.64 (d, $J = 7.7$ Hz, 2H, ArH), 5.32 (s, 2H, OCH_2), 3.69 (s, 6H, 2 \times OCH_3), 3.55 (s, 2H, ArCH_2N), 2.93-2.71 (m, 8H, 4 \times CH_2); ^{13}C NMR (75 MHz, $\text{DMSO-}d_6$) δ : 164.7, 152.7, 151.1, 148.2, 146.7, 144.8, 144.4, 139.4, 134.8, 134.8, 134, 128.8, 128.2, 127.7, 127.7, 126.8, 126.5, 124.2, 121.2, 120.3, 119.1, 112.3, 111.4, 108.3, 107.9, 72.3, 59.7, 58.0, 56.3, 56.1, 56.1, 33.4, 27.3; ESI-MS m/z : 580.3 $[\text{M}+\text{H}]^+$; IR (KBr, cm^{-1}) ν : 3115.04, 1665.08, 1257.55 (-CONH-), 2938.05, 1227.76 (- OCH_3), 1599.26, 1542.37, 1452.95, 1129.80, 754.01.

5.6.5

N-(2-((1-(4-(2-(6,7-dimethoxy-3,4-dihydroisoquinolin-2(1H)-yl)ethyl)phenyl)-1H-1,2,3-triazol-4-yl)methoxy)phenyl)-1H-indole-3-carboxamide (5)

Yield 49.6%; brown powder; mp: 157-159 °C; ^1H NMR (300 MHz, $\text{DMSO-}d_6$) δ : 11.82 (s, 1H, NH), 8.90 (s, 1H, CONH), 8.85 (s, 1H, NCH=C), 8.17-8.13 (m, 2H, ArH), 7.94 (d, $J = 7.8$ Hz, 1H, ArH), 7.73 (d, $J = 8.1$ Hz, 2H, ArH), 7.48 (s, 1H, ArH), 7.46-7.43 (m, 2H, ArH), 7.35 (d, $J = 8.0$ Hz, 1H, ArH), 7.16-6.94 (m, 4H, ArH), 6.65 (d, $J = 7.4$ Hz, 2H, ArH), 5.37 (s, 2H, OCH_2), 3.70 (s, 6H, 2 \times OCH_3), 3.35 (s, 2H, ArCH_2N), 3.18-2.72 (m, 8H, 4 \times CH_2); ^{13}C NMR (75 MHz, $\text{DMSO-}d_6$) δ : 164.7, 152.7, 148.2, 146.7, 144.4, 139.4, 138.6, 134.8, 134.8, 134.0, 130.7, 128.2, 128.2, 127.7, 126.8, 126.5, 124.2, 121.8, 121.7, 121.2, 120.3, 119.1, 112.8, 112.0, 111.4, 111.1, 108.3, 72.3, 59.7, 58.0,

56.3, 56.1, 56.1, 33.4, 27.3; ESI-MS m/z : 629.4 $[M+H]^+$; IR (KBr, cm^{-1}) ν : 3439.53, 1654.51, 1244.75 (-CONH-), 2938.05, 1229.02 (-OCH₃), 1518.43, 1449.65, 1129.30, 747.89

5.6.6

N-(2-((1-(4-(2-(6,7-dimethoxy-3,4-dihydroisoquinolin-2(1H)-yl)ethyl)phenyl)-1H-1,2,3-triazol-4-yl)methoxy)phenyl)benzofuran-2-carboxamide (6)

Yield 43.9%; brown powder; mp: 185-186 °C; ¹H NMR (300 MHz, DMSO-*d*₆) δ : 9.55 (s, 1H, CONH), 8.93 (s, 1H, NCH=C), 8.00 (s, 1H, ArH), 7.65 (s, 4H, ArH), 7.54 (m, 4H, ArH), 7.05 (s, 4H, ArH), 6.64 (s, 2H, ArH), 5.40 (s, 2H, OCH₂), 3.69 (s, 6H, 2 × OCH₃), 2.90 (s, 2H, ArCH₂N), 2.71 (m, 8H, 4 × CH₂); ¹³C NMR (75 MHz, DMSO-*d*₆) δ : 162.7, 157.2, 152.7, 150.0, 148.2, 146.7, 144.4, 139.4, 134.8, 134.8, 134.0, 128.2, 127.7, 127.7, 126.9, 126.8, 126.5, 124.7, 124.2, 123.3, 121.2, 120.9, 120.3, 119.1, 112.8, 111.5, 111.4, 108.9, 108.3, 72.3, 59.7, 58.0, 56.3, 56.1, 56.1, 33.4, 27.3; ESI-MS m/z : 630.5 $[M+H]^+$; IR (KBr, cm^{-1}) ν : 3392.40, 1681.31, 1255.42 (-CONH-), 2908.55, 1224.85 (-OCH₃), 1538.34, 1518.73, 1454.83, 1134.29, 753.85.

5.6.7

N-(2-((1-(4-(2-(6,7-dimethoxy-3,4-dihydroisoquinolin-2(1H)-yl)ethyl)phenyl)-1H-1,2,3-triazol-4-yl)methoxy)phenyl)-8-methoxy-4-oxo-1,4-dihydroquinoline-3-carboxamide (7)

Yield 61.9%; gray powder; mp: 139-141 °C; ¹H NMR (300 MHz, DMSO-*d*₆) δ : 10.03

(s, 1H, CONH), 8.92 (s, 1H, NCH=C), 8.87 (s, 1H, CH = C), 8.01 (d, $J = 7.6$ Hz, 1H, ArH), 7.78-7.69 (m, 4H, ArH), 7.46 (d, $J = 8.2$ Hz, 2H, ArH), 7.38-7.35 (m, 2H, ArH), 7.24 (t, $J = 7.5$, 1H, ArH), 7.06 (t, $J = 7.6$, 1H, ArH), 6.64 (d, $J = 6.3$ Hz, 2H, ArH), 5.33 (s, 2H, OCH₂), 4.00 (s, 3H, OCH₃), 3.70 (s, 6H, 2 × OCH₃), 3.46 (s, 2H, ArCH₂N), 2.94-2.71 (m, 8H, 4 × CH₂); ¹³C NMR (75 MHz, DMSO-*d*₆) δ: 174.5, 163.0, 156.7, 152.7, 148.2, 147.7, 146.7, 144.4, 139.4, 134.8, 134.8, 134.8, 134.0, 128.2, 127.7, 127.7, 126.8, 126.5, 124.2, 124.1, 121.2, 120.3, 119.1, 117.1, 112.8, 111.4, 108.3, 95.6, 72.3, 59.7, 58.0, 56.3, 56.1, 56.1, 55.9, 54.0, 46.0, 33.4, 27.3; ESI-MS *m/z*: 686.7 [M+H]⁺; IR (KBr, cm⁻¹) ν : 3445.43, 1670.84, 1270.60 (-CONH-), 2926.25, 1227.56 (-OCH₃), 1519.42, 1452.95, 1118.97, 748.91.

5.6.8

N-(2-((1-(4-(2-(6,7-dimethoxy-3,4-dihydroisoquinolin-2(1H)-yl)ethyl)phenyl)-1H-1,2,3-triazol-4-yl)methoxy)phenyl)thiophene-2-carboxamide (8)

Yield 76.9%; brown powder; mp: 160-162 °C; ¹H NMR (300 MHz, DMSO-*d*₆) δ: 9.57 (s, 1H, CONH), 8.84 (s, 1H, NCH=C), 7.97 (d, $J = 2.9$ Hz, 1H, ArH), 7.83 (d, $J = 4.9$ Hz, 1H, ArH), 7.77 (d, $J = 8.2$ Hz, 2H, ArH), 7.70 (d, $J = 7.7$ Hz, 1H, ArH), 7.50 (d, $J = 8.3$ Hz, 2H, ArH), 7.36 (d, $J = 8.1$ Hz, 1H, ArH), 7.24-7.18 (m, 2H, ArH), 7.03 (d, $J = 7.5$ Hz, 1H, ArH), 6.70 (d, $J = 9.4$ Hz, 2H, ArH), 5.35 (s, 2H, OCH₂), 3.82 (s, 2H, ArCH₂N), 3.72 (s, 6H, 2 × OCH₃), 3.00-2.83 (m, 8H, 4 × CH₂); ¹³C NMR (75 MHz, DMSO-*d*₆) δ: 161.8, 152.7, 148.2, 146.7, 144.4, 139.4, 139.4, 134.8, 134.8, 134.0, 131.9, 130.3, 129.0, 128.2, 127.7, 127.7, 126.8, 126.5, 124.2, 121.2, 120.3, 119.1, 112.8, 111.4, 108.3,

72.3, 59.7, 58.0, 56.3, 56.1, 56.1, 33.4, 27.3; ESI-MS m/z : 596.3 $[M+H]^+$; IR (KBr, cm^{-1})
 ν : 3410.03, 1650.26, 1255.30 (-CONH-), 2926.25, 1228.89 (-OCH₃), 1539.05, 1517.97,
1355.07, 1122.56, 743.12, 721.79.

5.6.9

N-(2-((1-(4-(2-(6,7-dimethoxy-3,4-dihydroisoquinolin-2(1H)-yl)ethyl)phenyl)-1H-1,2,3-triazol-4-yl)methoxy)phenyl)thiophene-3-carboxamide (9)

Yield 78.4%; brown powder; mp: 84-86 °C; ¹H NMR (300 MHz, DMSO-*d*₆) δ : 9.35 (s, 1H, CONH), 8.82 (s, 1H, NCH=C), 8.34 (s, 1H, ArH), 7.78-7.72 (m, 3H, ArH), 7.65-7.59 (m, 2H, ArH), 7.48 (d, J = 8.2 Hz, 2H, ArH), 7.36 (d, J = 8.1 Hz, 1H, ArH), 7.20 (t, J = 7.1 Hz, 1H, ArH), 7.00 (t, J = 7.5 Hz, 1H, ArH), 6.64 (d, J = 7.6 Hz, 2H, ArH), 5.34 (s, 2H, OCH₂), 3.70 (s, 6H, 2 × OCH₃), 3.40 (s, 4H, 2 × CH₂), 3.71 (s, 6H, 3 × CH₂); ¹³C NMR (75 MHz, DMSO-*d*₆) δ : 174.7, 152.7, 148.2, 146.7, 144.4, 139.4, 136.3, 134.8, 134.0, 129.0, 128.2, 127.7, 127.7, 127.6, 126.8, 126.6, 126.5, 124.2, 121.2, 120.3, 119.1, 112.8, 111.4, 108.3, 72.3, 59.7, 58.0, 56.3, 56.1, 56.1, 33.4, 27.3; ESI-MS m/z : 597.1 $[M+H]^+$; IR (KBr, cm^{-1}) ν : 3091.45, 1658.70, 1257.22 (-CONH-), 2926.25, 1227.88 (-OCH₃), 1533.09, 1517.75, 1128.25, 846.12, 751.56.

5.6.10

N-(2-((1-(4-(2-(6,7-dimethoxy-3,4-dihydroisoquinolin-2(1H)-yl)ethyl)phenyl)-1H-1,2,3-triazol-4-yl)methoxy)phenyl)-3-methylthiophene-2-carboxamide (10)

Yield 52.4%; brown powder; mp: 163-165 °C; ¹H NMR (300 MHz, DMSO-*d*₆) δ :

8.92 (s, 1H, CONH), 8.83 (s, 1H, NCH=C), 8.10 (d, $J = 7.5$ Hz, 1H, ArH), 7.78 (d, $J = 7.3$ Hz, 2H, ArH), 7.66 (d, $J = 4.0$ Hz, 1H, ArH), 7.49 (d, $J = 7.1$ Hz, 2H, ArH), 7.35 (d, $J = 7.4$ Hz, 1H, ArH), 7.17 (s, 1H, ArH), 7.04-6.99 (m, 2H, ArH), 6.64 (d, $J = 6.9$ Hz, 2H, ArH), 5.35 (s, 2H, OCH₂), 3.93 (s, 6H, 2 × OCH₃), 3.55 (s, 2H, CH₂), 2.91 (s, 2H, CH₂), 2.71 (s, 6H, 3 × CH₂), 2.36 (s, 3H, CH₃); ¹³C NMR (75 MHz, DMSO-*d*₆) δ : 161.8, 152.7, 148.2, 146.7, 144.4, 139.4, 136.3, 135.0, 134.8, 134.8, 134.0, 129.2, 128.2, 127.7, 127.7, 126.8, 126.5, 124.5, 124.2, 121.2, 120.3, 119.1, 112.8, 111.4, 108.3, 72.3, 59.7, 58.0, 56.3, 56.1, 56.1, 33.4, 27.3, 13.7; ESI-MS m/z : 610.8 [M+H]⁺; IR (KBr, cm⁻¹) ν : 3427.73, 1638.00, 1251.86 (-CONH-), 2926.25, 1227.55 (-OCH₃), 1536.27, 1518.12, 1125.48, 756.40, 743.31.

5.6.11

N-(2-((1-(4-(2-(6,7-dimethoxy-3,4-dihydroisoquinolin-2(1H)-yl)ethyl)phenyl)-1H-1,2,3-triazol-4-yl)methoxy)phenyl)-5-methylthiophene-2-carboxamide (11)

Yield 50.1%; brown powder; mp: 146-147 °C; ¹H NMR (300 MHz, DMSO-*d*₆) δ : 9.40 (s, 1H, CONH), 8.81 (s, 1H, NCH=C), 7.74 (s, 4H, ArH), 7.49 (s, 2H, ArH), 7.34 (m, 1H, ArH), 7.20 (m, 1H, ArH), 7.01 (m, 1H, ArH), 6.88 (s, 1H, ArH), 6.65 (m, 2H, ArH), 5.34 (s, 2H, OCH₂), 3.70 (s, 6H, 2 × OCH₃), 3.56 (s, 2H, CH₂), 2.90 (s, 2H, CH₂), 2.71 (s, 6H, 3 × CH₂), 2.46 (s, 3H, CH₃); ¹³C NMR (75 MHz, DMSO-*d*₆) δ : 161.8, 152.9, 152.7, 148.2, 146.7, 144.4, 139.4, 135.3, 134.8, 134.8, 134.0, 129.5, 128.5, 128.2, 127.7, 127.7, 126.8, 126.5, 124.2, 121.2, 120.3, 119.1, 112.8, 111.4, 108.3, 72.3, 59.7, 58.0, 56.3, 56.1, 33.4, 27.3, 14.5; ESI-MS m/z : 610.7 [M+H]⁺; IR (KBr, cm⁻¹) ν : 3415.93,

1655.91, 1254.81 (-CONH-), 2932.15, 1227.35 (-OCH₃), 1521.96, 1450.91, 1128.87, 738.78.

5.6.12

5-chloro-N-(2-((1-(4-(2-(6,7-dimethoxy-3,4-dihydroisoquinolin-2(1H)-yl)ethyl)phenyl)l)-1H-1,2,3-triazol-4-yl)methoxy)phenyl)thiophene-2-carboxamide (12)

Yield 79.4%; brown powder; mp: 128-130 °C; ¹H NMR (300 MHz, DMSO-*d*₆) δ: 9.73 (s, 1H, CONH), 8.80 (s, 1H, NCH=C), 7.86 (d, *J* = 2.8 Hz, 1H, ArH), 7.74 (d, *J* = 7.6 Hz, 2H, ArH), 7.61 (d, *J* = 7.5 Hz, 1H, ArH), 7.48 (d, *J* = 7.6 Hz, 2H, ArH), 7.37 (d, *J* = 7.9 Hz, 1H, ArH), 7.23 (t, *J* = 9.0 Hz, 2H, ArH), 7.02 (t, *J* = 7.5 Hz, 1H, ArH), 6.64 (d, *J* = 7.2 Hz, 2H, ArH), 5.33 (s, 2H, OCH₂), 3.70 (s, 6H, 2 × OCH₃), 3.56 (s, 2H, CH₂), 2.90 (s, 2H, CH₂), 2.71 (s, 6H, 3 × CH₂); ¹³C NMR (75 MHz, DMSO-*d*₆) δ: 161.8, 152.7, 148.2, 146.7, 144.4, 140.7, 139.4, 138.3, 135.9, 134.8, 134.8, 134.0, 129.8, 128.2, 127.7, 127.7, 126.8, 126.5, 124.2, 121.2, 120.3, 119.1, 112.8, 111.4, 108.3, 72.3, 59.7, 58.0, 56.3, 56.1, 56.1, 33.4, 27.3; ESI-MS *m/z*: 630.7 [M+H]⁺; IR (KBr, cm⁻¹) ν: 3345.13, 1657.42, 1255.05 (-CONH-), 2926.25, 1229.30 (-OCH₃), 1541.17, 1518.72, 1453.45, 1130.33, 745.36.

5.9 Materials and methods

5.9.1 Materials

Adriamycin (ADM), verapamil (VRP), 3-(4, 5-dimethylthiazol-2-yl)-2, 5-diphenyl tetrazolium bromide (MTT), and DMSO were purchased from Sigma-Aldrich (St. Louis,

MO, USA). WK-X-34 with high purity was synthesized by our laboratory before ^[20]. All other chemicals were molecular biology grade and obtained from Sigma-Aldrich or Thermo Fisher Scientific (Waltham, MA, USA).

5.9.2 Cell lines and cell culture

Human leukemia cell line K562 and its adriamycin-selected P-gp-overexpressing subline K562/A02 were kindly provided by Dr. Dr. Yun-Man Li (Department of Physiology, China Pharmaceutical University, Nanjing, China). The cell lines were grown in RPMI-1640 medium containing 10% fetal bovine serum (FBS) and incubated at 37 °C in a humidified incubator with 5% CO₂ in air growth. To maintain MDR phenotype, 1 mg/mL adriamycin was added to K562/A02 cultures and maintained in drug-free medium for 2 weeks before use. All experiments were performed with cells in exponential growth. To maintain MDR phenotype, 1 mg/mL adriamycin was added to the K562/A02 cultures and maintained in a drug-free medium for 2 weeks before use.

5.9.3 MTT assay

K562/A02 cells were incubated in RPMI 1640 medium supplemented with 10% fetal bovine serum at 37 °C in a 5% CO₂ humidified atmosphere. K562/A02 cells (1-2 × 10⁴ cells per well) were seeded in 96-well plates. After 24 h incubation, cells were treated with various concentrations of ADM in absence or presence of target compounds for 48 h in an atmosphere of 95% air with 5% CO₂ at 37 °C. Then, MTT

was added directly to the cells. After additional incubation for 4 h at 37°C, the absorbance at 570 nm was read on a microplate reader (Thermo Fisher Scientific). The IC₅₀ values of the compounds for cytotoxicity were calculated by GraphPad Prism 5.0 software from the dose–response curves. Experiments were conducted in triplicates and repeated three times independently.

5.9.4 Duration of the MDR reversal

1-2 × 10⁴ K562/A02 cells per well were plated in 96-well plates and cultured overnight, then the cells were incubated for another 24 h with or without compound **11**, VRP, WK-X-34 or PBS at the concentration of 5 μM before being washed 0 or 3 times with growth medium. Then, the cells were incubated for 0, 6, 12 or 24 h before the addition of various concentrations of ADM or vehicle. The incubation was continued for 48 h prior to the MTT analysis. The IC₅₀ values of the compounds for cytotoxicity were calculated by GraphPad Prism 5.0 software from the dose–response curves.

5.9.5 Accumulation of ADM

ADM accumulation assay was performed according to the reported procedures with minor modification^[26]. In brief, 2 × 10⁵ cells of K562 and K562/A02 were incubated with 20 μM ADM and different concentrations of compound **11** for 2.5 h at 37 °C. 0.1% DMSO was used as a negative control. VRP and WK-X-34 were used as positive controls. After incubation, the cells were washed with cold PBS and lysed

with lysis buffer (0.75 M HCl, 0.2% Triton-X100 in isopropanol). The fluorescence level of ADM in the lysate was determined by fluorescence spectrophotometer (RF-5301 PC; Shimadzu) using an excitation and an emission wavelength pair of 460 and 610 nm. Accumulation was expressed as ADM fluorescent intensity (FI) per 2×10^5 cells. All incubations were carried out in triplicate and three independent experiments were performed.

5.9.6. Rhodamine123 efflux assay

K562 or K562/A02 cells were seeded into 24-well plates at 1.5×10^5 /well and incubated with 5 μ M Rh123 for 60 min before washing with ice PBS for three times. Then the cells were incubated with or without various concentrations of compound **11**, WK-X-34 or VRP (1.0, 2.5, 5 μ M) for another 90 min. Afterwards the cells were washed twice in ice-cold PBS. The mean fluorescence intensity of retained intracellular Rh123 was estimated by BD FACSCalibur flow cytometer.

Acknowledgments

This work was supported by the National Science and Technology Major Project of the Ministry of Science and Technology of China (NO. 2009ZX09102-033) and National Natural Science Foundation of China (NO. 81173088).

Notes and references

Author information. ^a Center of Drug Discovery, State Key Laboratory of Natural

Medicines,, China Pharmaceutical University, 24 TongjiXiang, Nanjing 210009, P. R. China. ^b Jiangsu Key Laboratory of Drug Discovery for Metabolic Disease, China Pharmaceutical University, 24 TongjiXiang, Nanjing 210009, P. R. China.

Corresponding authors.*Wenglong Huang: phone: +86-25-83271302; fax: +86-25-83271302; E-mail: ydhuangwenlong@126.com; *Hai Qian: phone: +86-25-83271302; fax: +86-25-83271320; E-mail: qianhai24@163.com.

Conflict of interest. All authors report no conflict of interest.

References

- [1] T. Fojo, M. Menefee, *Ann Oncol*, 2007, **18**, v3-v8.
- [2] P.D. Eckford, F.J. Sharom, *Chem Rev*, 2009, **109**, 2989-3011.
- [3] M. Susa, E. Choy, C. Yang, J. Schwab, H. Mankin, F. Hornicek, Z. Duan, *J Biomol Screen*, 2010, **15**, 287-296.
- [4] G. Szakacs, J.K. Paterson, J.A. Ludwig, C. Booth-Genthe, M.M. Gottesman, *Nat Rev Drug Discov*, 2006, **5**, 219-234.
- [5] A. Breier, L. Gibalova, M. Seres, M. Barancik, Z. Sulova, *Anti-Cancer Agents in Medicinal Chemistry (Formerly Current Medicinal Chemistry-Anti-Cancer Agents)*, 2013, **13**, 159-170.
- [6] B.I. Sikic, *Oncology (Williston Park, NY)*, 1999, **13**, 183-187.
- [7] C. Martelli, D. Alderighi, M. Coronello, S. Dei, M. Frosini, B. Le Bozec, D. Manetti, A. Neri, M.N. Romanelli, M. Salerno, *J Med Chem*, 2009, **52**, 807-817.
- [8] A. Mihályi, R. Gáspár, Z. Zalán, L. Lázár, F. Fülöp, P.A. de Witte, *Anticancer Res*, 2004, **24**, 1631-1636.

- [9] F. Sharom, *J Membrane Biol*, 1997, **160**, 161-175.
- [10] P. Ruff, D.A. Vorobiof, J.P. Jordaan, G.S. Demetriou, S.D. Moodley, A.L. Nosworthy, I.D. Werner, J. Raats, L.J. Burgess, *Cancer Chemother Pharmacol*, 2009, **64**, 763-768.
- [11] J. Robert, C. Jarry, *J Med Chem*, 2003, **46**, 4805-4817.
- [12] L. Zhang, S. Ma, *ChemMedChem*, 2010, **5**, 811-822.
- [13] H.Y. Hung, E. Ohkoshi, M. Goto, K. Nakagawa-Goto, K.H. Lee, *Bioorg Med Chem Lett*, 2012, **22**, 7726-7729.
- [14] M.J. Henderson, M. Haber, A. Porro, M.A. Munoz, N. Iraci, C. Xue, J. Murray, C.L. Flemming, J. Smith, J.I. Fletcher, S. Gherardi, C.K. Kwek, A.J. Russell, E. Valli, W.B. London, A.B. Buxton, L.J. Ashton, A.C. Sartorelli, S.L. Cohn, M. Schwab, G.M. Marshall, G. Perini, M.D. Norris, *J Natl Cancer Inst*, 2011, **103**, 1236-1251.
- [15] V. Jekerle, W. Klinkhammer, R.M. Reilly, M. Piquette-Miller, M. Wiese, *Cancer Chemother Pharmacol*, 2007, **59**, 61-69.
- [16] R.Z. Pellicani, A. Stefanachi, M. Niso, A. Carotti, F. Leonetti, O. Nicolotti, R. Perrone, F. Berardi, S. Cellamare, N.A. Colabufo, *J Med Chem*, 2012, **55**, 424-436.
- [17] M. Wijtmans, C. de Graaf, G. de Kloe, E.P. Istyastono, J. Smit, H. Lim, R. Boonak, S. Nijmeijer, R.A. Smits, A. Jongejan, O. Zuiderveld, I.J. de Esch, R. Leurs, *J Med Chem*, 2011, **54**, 1693-1703.
- [18] H.C. Kolb, K.B. Sharpless, *Drug Discov Today*, 2003, **8**, 1128-1137.
- [19] X. Gu, Z. Ren, X. Tang, H. Peng, Q. Zhao, Y. Lai, S. Peng, Y. Zhang, *Eur J Med Chem*, 2012, **51**, 137-144.
- [20] B. Liu, Q. Qiu, T. Zhao, L. Jiao, J. Hou, Y. Li, H. Qian, W. Huang, *Chemical biology &*

drug design, 2014, **84**, 182-191.

[21] X. Tang, X. Gu, Z. Ren, Y. Ma, Y. Lai, H. Peng, S. Peng, Y. Zhang, *Bioorg Med Chem Lett*, 2012, **22**, 2675-2680.

[22] M.J. Newman, J.C. Rodarte, K.D. Benbatoul, S.J. Romano, C. Zhang, S. Krane, E.J. Moran, R.T. Uyeda, R. Dixon, E.S. Guns, *Cancer Res*, 2000, **60**, 2964-2972.

[23] Y. Gong, Y. Wang, F. Chen, J. Han, J. Miao, N. Shao, Z. Fang, R.O. Yang, *Leukemia Res*, 2000, **24**, 769-774.

[24] Y.-q. Shi, X.-j. Qu, Y.-x. Liao, C.-f. Xie, Y.-n. Cheng, S. Li, H.-x. Lou, *Eur J Pharmacol*, 2008, **584**, 66-71.

[25] B.-S. Ji, L. He, G.-Q. Liu, *Life Sci*, 2005, **77**, 2221-2232.

[26] K.-F. Chan, I.L. Wong, J.W. Kan, C.S. Yan, L.M. Chow, T.H. Chan, *J Med Chem*, 2012, **55**, 1999-2014.

Figure caption

Fig. 1 Structures of Verapamil, VX-710, Zosuquidar and Tariquidar

Fig. 2 Structure of WK-X-34 and design of the target compounds

Scheme 1 Synthesis of the target compounds. Reagents and conditions: (i) 3-bromoprop-1-yne, K_2CO_3 , acetone, reflux, 3 h; (ii) Fe/NH_4Cl , 80% EtOH, reflux, 2.5 h; (iii) heterocyclic aromatic acyl chlorides, TEA/DCM, r.t., 24 h; or heterocyclic aromatic formic acids, EDC·HCl/DMAP/DCM, r.t., 48 h; (iv) 1-(2-bromoethyl)-4-nitrobenzene, K_2CO_3 , acetonitrile, reflux, 17 h; (v) $H_2/Pd/C$, DCM/EtOH, r.t., 24 h; (vi) $NaNO_2$, 50% AcOH, 0-5 °C, 30 min; NaN_3 , 0-5 °C, 50 min; (vii) **c1-c12**, ascorbate sodium, $CuSO_4$, 75%CH₃OH, 24-48 h.

Table 1 Cytotoxicity of the target compounds against K562 and K562/A02 cell lines. The IC₅₀s for the target compounds were determined by MTT method. Each experiment was carried out three times.

Table 2 ADM-resistance reversal activity of the target compounds **1-12** at 5 μM concentration in K562/A02 cells. The IC₅₀ value was determined after exposure to a series of ADM concentration with different target compounds at 5 μM using K562/A02 cells. Reversal fold (RF) refers to fold-change in drug sensitivity. RF= (IC₅₀ without modulator)/ (IC₅₀ with 5 μM modulator). 0.1% DMSO was added as solvent control for testing the P-gp modulating activity.

Table 3 Sensitization of compound **11** on reversing MDR towards K562/A02 cells at different concentrations. Data were analyzed with GraphPad Prism 5.0 software and are the mean ± SD for 3 independent tests. The IC₅₀ of ADM was 82.21 ± 3.7 μM. Reversal fold (RF), RF= (IC₅₀ without modulator)/ (IC₅₀ with modulator).

Fig. 3 EC₅₀ for the compound **11** in K562/A02 cells. Various concentrations (0.10, 0.25, 0.50, 1.00, 2.50, 5.00, 10.00, 20.00 μM) of compound **11** and ADM were added to 96-well plates and the cells were incubated for 48 h. The absorption values were measured with a Microplate Reader at 490 nm. Data were analyzed with GraphPad Prism 5.0 software and are the mean ± SD for 3 independent tests.

Table 4 Duration of MDR reversal in K562/A02 cells after incubation and washout of P-gp inhibitor. Numbers in parentheses, Reversal fold (RF), RF= (IC₅₀ without modulator)/ (IC₅₀ with modulator). Each experiment was carried out two to three times, and the values were presented as the mean ± standard error of mean. Nd: not

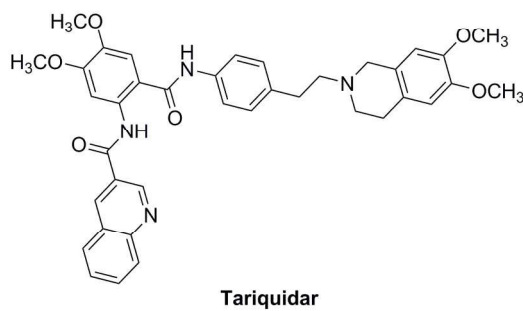
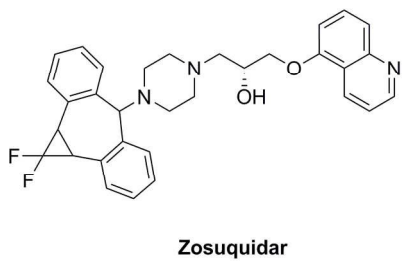
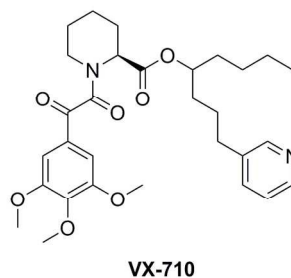
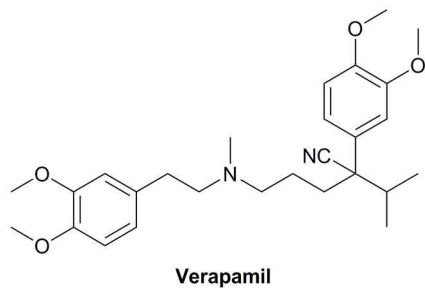
determined.

Fig. 4 Effect of compound **11** on intracellular ADM accumulation in K562/A02 cells.

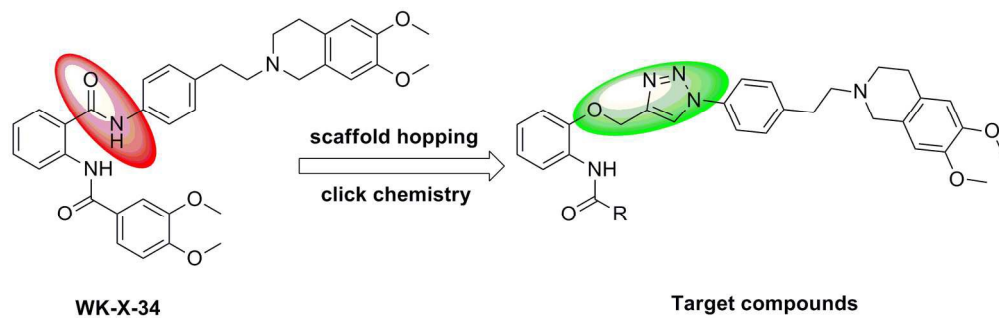
0.1% DMSO was used as negative control. VRP and WK-X-34 were chosen as positive controls. The mean fluorescence intensity of retained intracellular ADM was estimated by spectrofluorometry. Data were expressed as means \pm S.D. of 3 independent experiments. *P<0.05, **P<0.01 vs. untreated K562/A02 cells.

Fig. 5. Inhibitory effect of compound **11** on the efflux of Rh123. K562 or K562/A02

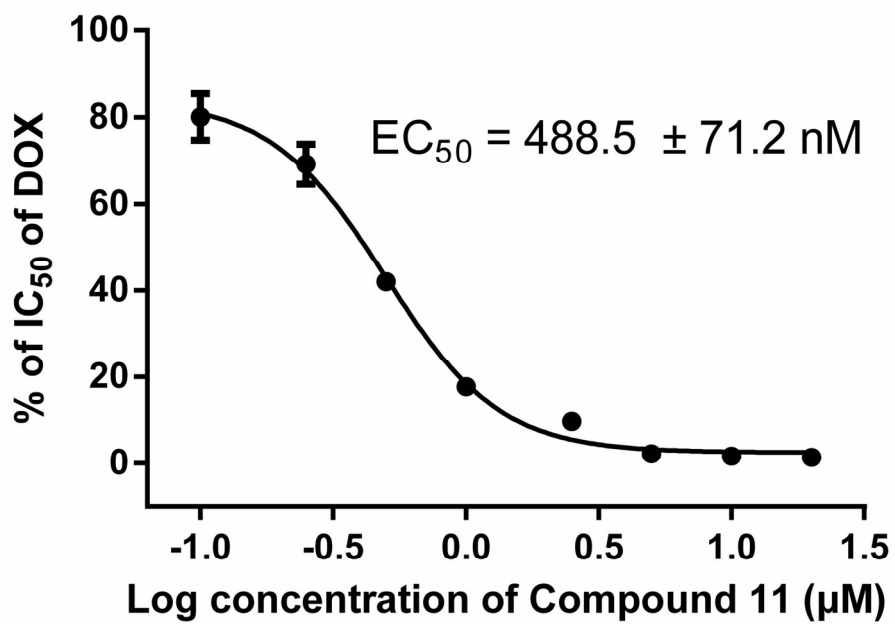
cells were incubated with 5 μ M Rh123 for 60 min. Then various concentrations of compound **11**, WK-X-34 or VRP (1.0, 2.5, 5 μ M) was added and the cells were incubated for a further 90 min. Afterwards the cells were washed 3 times in ice-cold PBS. The mean fluorescence intensity of retained intracellular Rh123 was estimated by flow cytometry. Data were expressed as means \pm S.D. of 3 independent experiments. *P<0.05, **P<0.01 vs. untreated K562/A02 cells.



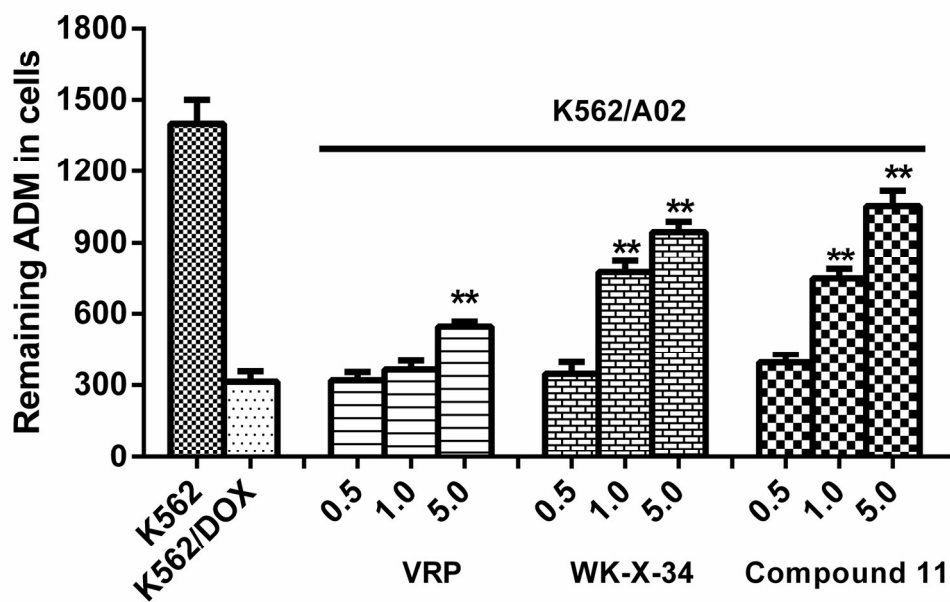
176x124mm (300 x 300 DPI)



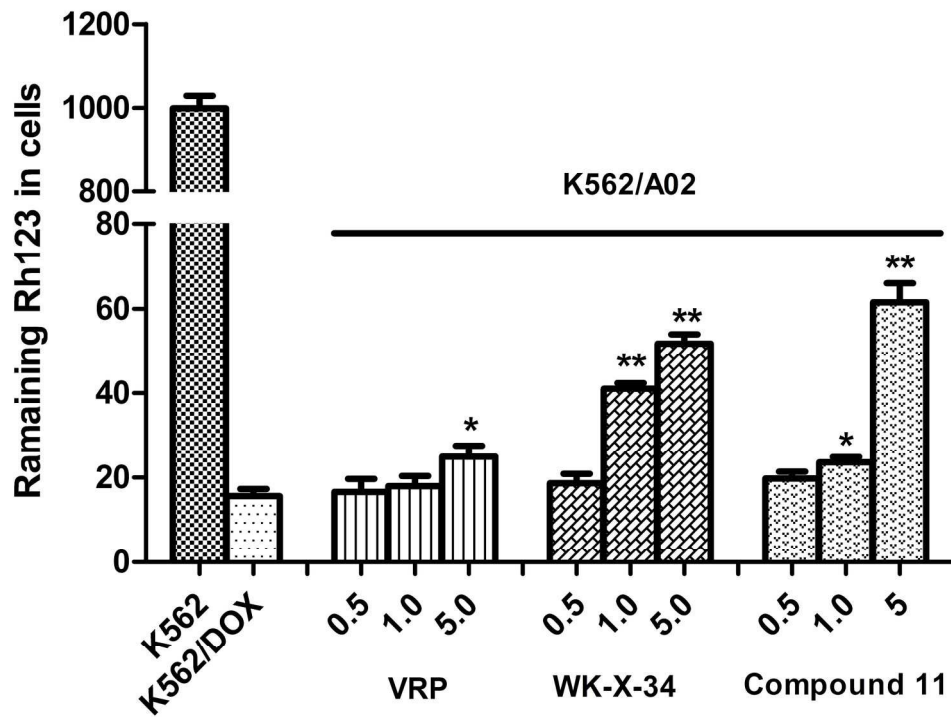
169x53mm (300 x 300 DPI)



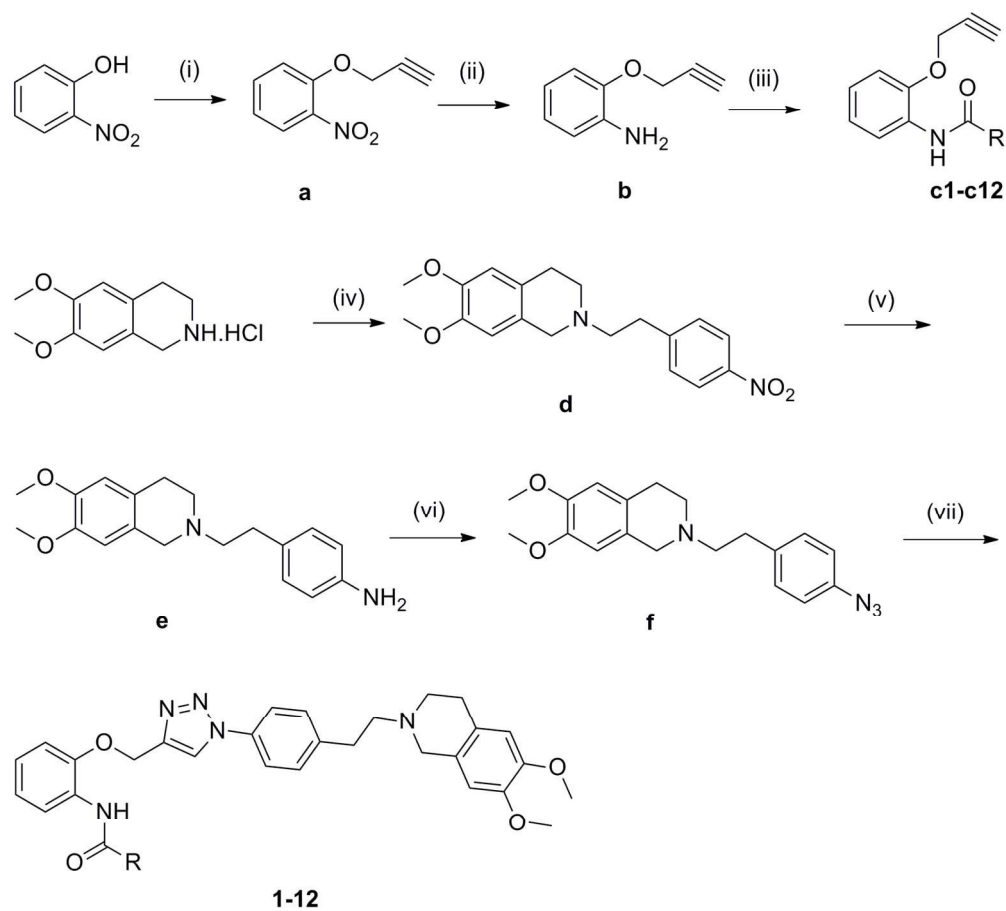
73x51mm (600 x 600 DPI)



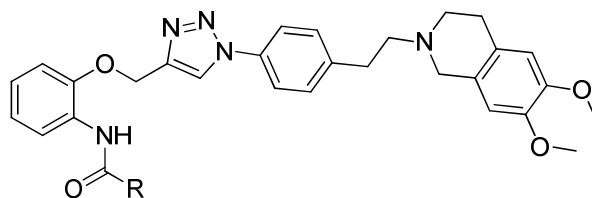
80x54mm (600 x 600 DPI)



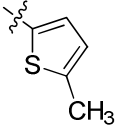
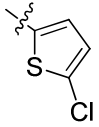
92x71mm (600 x 600 DPI)



148x135mm (300 x 300 DPI)

Table. 1 Cytotoxicity of the target compounds against K562 and K562/A02 cell lines

Compounds	R'	IC ₅₀ of ADM (μM)	IC ₅₀ of ADM/A02 (μM)
1		>100	>100
2		>100	>100
3		>100	>100
4		>100	>100
5		17.2 ± 1.3	19.6 ± 2.1
6		>100	>100
7		23.3 ± 1.7	16.3 ± 1.5
8		>100	>100
9		>100	>100
10		>100	>100

11		>100	>100
12		>100	>100
WK-X-34		6.9 ± 1.9	33.7 ± 2.7
VRP		41.6 ± 2.7	37.2 ± 3.2
ADM		0.47 ± 0.03	71.04 ± 3.2

The IC_{50} s for the target compounds were determined by MTT method. Each experiment was carried out three times.

Table. 2 ADM-resistance reversal activity of the target compounds **1-12** at 5 μ M concentration in K562/A02 cells

Compounds	IC ₅₀ of ADM (μ M)	RF
1	13.36 \pm 1.0	5.3
2	8.95 \pm 0.5	7.9
3	4.76 \pm 0.4	14.9
4	4.12 \pm 0.3	17.2
5	13.42 \pm 1.4	5.3
6	15.06 \pm 0.9	4.7
7	4.4 \pm 0.3	16.1
8	4.21 \pm 0.2	16.9
9	16.92 \pm 1.3	4.2
10	4.05 \pm 0.2	17.5
11	1.76 \pm 0.3	40.4
12	8.96 \pm 0.7	7.9
WK-X-34	2.31 \pm 0.3	30.8
VRP	17.13 \pm 1.7	4.1
Control	71.04 \pm 3.2	1.0

The IC₅₀ value was determined after exposure to a series of ADM concentration with different target compounds at 5 μ M using K562/A02 cells. Reversal fold (RF) refers to fold-change in drug sensitivity. RF= (IC₅₀ without modulator)/ (IC₅₀ with 5 μ M modulator).0.1% DMSO was added as solvent control for testing the P-gp modulating activity.

Table 3: Sensitization of compound **11** on reversing MDR towards K562/A02 cells at different concentrations

Compounds 11	IC ₅₀ of ADM (μ M)	RF
0.1	80.07 \pm 9.3	1.0
0.25	69.21 \pm 8.00	1.2
0.5	42.00 \pm 1.16	2.0
1	17.75 \pm 1.7	4.6
2.5	9.75 \pm 0.25	8.4
5	2.26 \pm 0.05	36.3
10	1.65 \pm 0.03	49.9
20	1.41 \pm 0.01	58.4

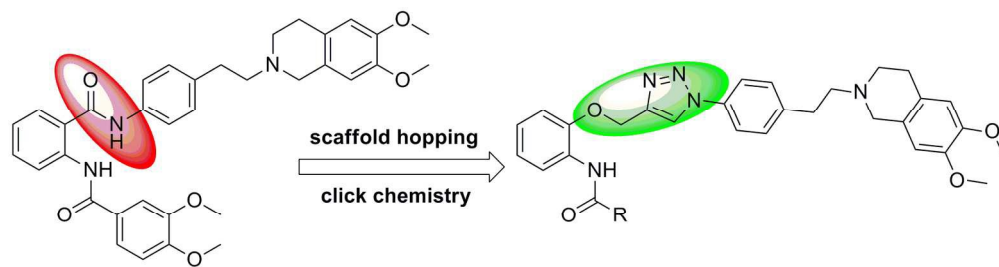
Data were analyzed with GraphPad Prism 5.0 software and are the mean \pm SD for 3 independent tests. The IC₅₀ of ADM was 82.21 \pm 3.7 μ M. Reversal fold (RF), RF= (IC₅₀ without modulator)/ (IC₅₀ with modulator).

Table 4: Duration of MDR reversal in K562/A02 cells after incubation and washout of

P-gp inhibitor

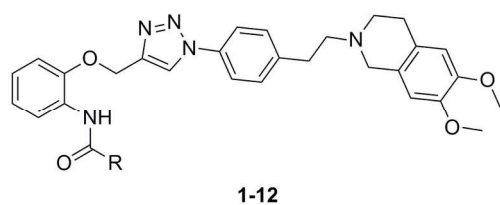
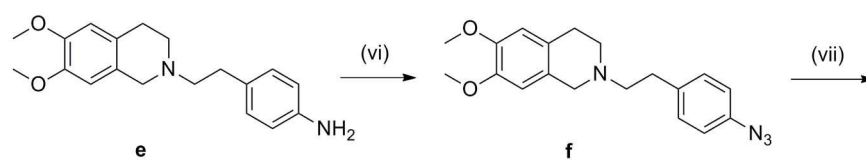
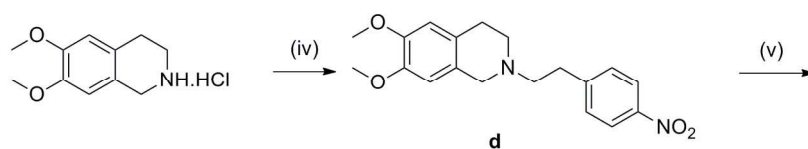
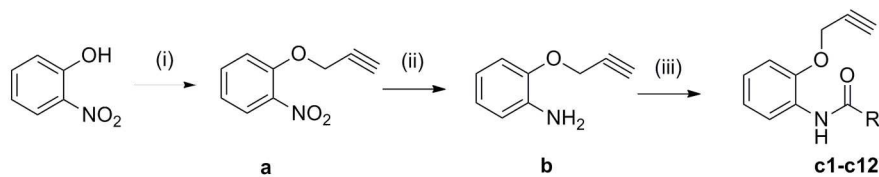
Treatment schedule	IC ₅₀ /ADM[μ M] (RF)			
	Control	VRP (5 μ M)	WK-X-34(5 μ M)	Compound 11(5 μ M)
No wash	79.86 \pm 2.25 (1)	19.32 \pm 1.3(3.7)	2.32 \pm 0.3(34.4)	2.11 \pm 0.2(37.8)
Wash, 0h	nd	51.17 \pm 6.3(1.6)	3.71 \pm 0.3(21.5)	4.31 \pm 0.3(18.5)
Wash, 6h	nd	nd	6.43 \pm 0.2(12.4)	9.42 \pm 0.7(8.5)
Wash, 12h	nd	nd	9.65 \pm 0.5(8.3)	17.17 \pm 1.6(4.7)
Wash, 24h	nd	nd	12.91 \pm 0.7(6.2)	32.41 \pm 1.9(2.5)

Numbers in parentheses, Reversal fold (RF), RF= (IC₅₀without modulator)/ (IC₅₀with modulator). Each experiment was carried out two to three times, and the values were presented as the mean \pm standard error of mean. Nd: not determined.



WK-X-34

Target compounds



1-12

169x191mm (300 x 300 DPI)